

Chapter 4

Dynamical Equations for Flight Vehicles

These notes provide a systematic background of the derivation of the equations of motion for a flight vehicle, and their linearization. The relationship between dimensional stability derivatives and dimensionless aerodynamic coefficients is presented, and the principal contributions to all important stability derivatives for flight vehicles having left/right symmetry are explained.

4.1 Basic Equations of Motion

The equations of motion for a flight vehicle usually are written in a body-fixed coordinate system. It is convenient to choose the vehicle center of mass as the origin for this system, and the orientation of the (right-handed) system of coordinate axes is chosen by convention so that, as illustrated in Fig. 4.1:

- the x -axis lies in the symmetry plane of the vehicle¹ and points forward;
- the z -axis lies in the symmetry plane of the vehicle, is perpendicular to the x -axis, and points down;
- the y -axis is perpendicular to the symmetry plane of the vehicle and points out the right wing.

The precise orientation of the x -axis depends on the application; the two most common choices are:

- to choose the orientation of the x -axis so that the product of inertia

$$I_{xz} = \int_m xz \, dm = 0$$

¹Almost all flight vehicles have bi-lateral (or, left/right) symmetry, and most flight dynamics analyses take advantage of this symmetry.

The other products of inertia, I_{xy} and I_{yz} , are automatically zero by vehicle symmetry. When all products of inertia are equal to zero, the axes are said to be *principal axes*.

- to choose the orientation of the x -axis so that it is parallel to the velocity vector for an initial equilibrium state. Such axes are called *stability axes*.

The choice of principal axes simplifies the moment equations, and requires determination of only one set of moments of inertia for the vehicle – at the cost of complicating the X - and Z -force equations because the axes will not, in general, be aligned with the lift and drag forces in the equilibrium state. The choice of stability axes ensures that the lift and drag forces in the equilibrium state are aligned with the Z and X axes, at the cost of additional complexity in the moment equations and the need to re-evaluate the inertial properties of the vehicle (I_x , I_z , and I_{xz}) for each new equilibrium state.

4.1.1 Force Equations

The equations of motion for the vehicle can be developed by writing Newton's second law for each differential element of mass in the vehicle,

$$d\vec{F} = \vec{a} dm \quad (4.1)$$

then integrating over the entire vehicle. When working out the acceleration of each mass element, we must take into account the contributions to its velocity from both linear velocities (u, v, w) in each of the coordinate directions as well as the $\vec{\Omega} \times \vec{r}$ contributions due to the rotation rates (p, q, r) about the axes. Thus, the time rates of change of the coordinates in an inertial frame instantaneously coincident with the body axes are

$$\begin{aligned} \dot{x} &= u + qz - ry \\ \dot{y} &= v + rx - pz \\ \dot{z} &= w + py - qx \end{aligned} \quad (4.2)$$

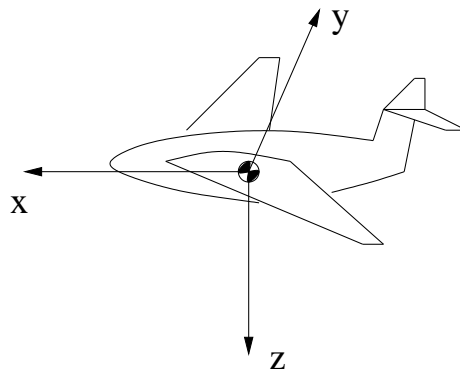


Figure 4.1: Body axis system with origin at center of gravity of a flight vehicle. The x - z plane lies in vehicle symmetry plane, and y -axis points out right wing.

and the corresponding accelerations are given by

$$\begin{aligned}\ddot{x} &= \frac{d}{dt}(u + qz - ry) \\ \ddot{y} &= \frac{d}{dt}(v + rx - pz) \\ \ddot{z} &= \frac{d}{dt}(w + py - qx)\end{aligned}\tag{4.3}$$

or

$$\begin{aligned}\ddot{x} &= \dot{u} + \dot{q}z + q(w + py - qx) - \dot{r}y - r(v + rx - pz) \\ \ddot{y} &= \dot{v} + \dot{r}x + r(u + qz - ry) - \dot{p}z - p(w + py - qx) \\ \ddot{z} &= \dot{w} + \dot{p}y + p(v + rx - pz) - \dot{q}x - q(u + qz - ry)\end{aligned}\tag{4.4}$$

Thus, the net product of mass times acceleration for the entire vehicle is

$$\begin{aligned}m\vec{a} &= \int_m \{[\dot{u} + \dot{q}z + q(w + py - qx) - \dot{r}y - r(v + rx - pz)]\hat{i} + \\ &\quad [\dot{v} + \dot{r}x + r(u + qz - ry) - \dot{p}z - p(w + py - qx)]\hat{j} + \\ &\quad [\dot{w} + \dot{p}y + p(v + rx - pz) - \dot{q}x - q(u + qz - ry)]\hat{k}\} dm\end{aligned}\tag{4.5}$$

Now, the velocities and accelerations, both linear and angular, are constant during the integration over the vehicle coordinates, so the individual terms in Eq. (4.5) consist of integrals of the form

$$\int_m dm = m$$

which integrates to the vehicle mass m , and

$$\int_m x dm = \int_m y dm = \int_m z dm = 0,\tag{4.6}$$

which are all identically zero since the origin of the coordinate system is at the vehicle center of mass. Thus, Eq. (4.5) simplifies to

$$m\vec{a} = m [(\dot{u} + qw - rv)\hat{i} + (\dot{v} + ru - pw)\hat{j} + (\dot{w} + pv - qu)\hat{k}]\tag{4.7}$$

To write the equation corresponding to Newton's Second Law, we simply need to set Eq. (4.7) equal to the net external force acting on the vehicle. This force is the sum of the aerodynamic (including propulsive) forces and those due to gravity.

In order to express the gravitational force acting on the vehicle in the body axis system, we need to characterize the orientation of the body axis system with respect to the gravity vector. This orientation can be specified using the *Euler angles* of the body axis system with respect to an inertial system (x_f, y_f, z_f) , where the inertial system is oriented such that

- the z_f axis points down (i.e., is parallel to the gravity vector \vec{g});
- the x_f axis points North; and
- the y_f axis completes the right-handed system and, therefore, points East.

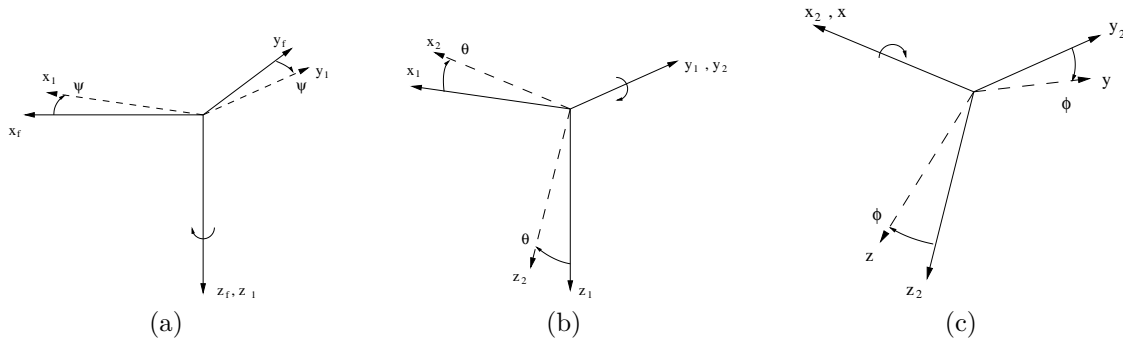


Figure 4.2: The Euler angles Ψ , Θ , and Φ determine the orientation of the body axes of a flight vehicle. (a) Yaw rotation about z -axis, nose right; (b) Pitch rotation about y -axis, nose up; (c) Roll rotation about x -axis, right wing down.

The orientation of the body axis system is specified by starting with the inertial system, then, *in the following order* performing:

1. a positive rotation about the z_f axis through the heading angle Ψ to produce the (x_1, y_1, z_1) system; then
2. a positive rotation about the y_1 axis through the pitch angle Θ to produce the (x_2, y_2, z_2) system; and, finally
3. a positive rotation about the x_2 axis through the bank angle Φ to produce the (x, y, z) system.

Thus, if we imagine the vehicle oriented initially with its z -axis pointing down and heading North, its final orientation is achieved by rotating through the heading angle Ψ , then pitching up through angle Θ , then rolling through angle Φ . This sequence of rotations is sketched in Fig. 4.2.

Since we are interested only in the orientation of the gravity vector in the body axis system, we can ignore the first rotation.² Thus, we need consider only the second rotation, in which the components of any vector transform as

$$\begin{pmatrix} x_2 \\ y_2 \\ z_2 \end{pmatrix} = \begin{pmatrix} \cos \Theta & 0 & -\sin \Theta \\ 0 & 1 & 0 \\ \sin \Theta & 0 & \cos \Theta \end{pmatrix} \begin{pmatrix} x_f \\ y_f \\ z_f \end{pmatrix} \quad (4.8)$$

and the third rotation, in which the components transform as

$$\begin{pmatrix} x \\ y \\ z \end{pmatrix} = \begin{pmatrix} 1 & 0 & 0 \\ 0 & \cos \Phi & \sin \Phi \\ 0 & -\sin \Phi & \cos \Phi \end{pmatrix} \begin{pmatrix} x_2 \\ y_2 \\ z_2 \end{pmatrix} \quad (4.9)$$

²If we are interested in determining where the vehicle is going – say, we are planning a flight path to get us from New York to London, we certainly are interested in the heading, but this is not really an issue as far as analysis of the stability and controllability of the vehicle are concerned.

Thus, the rotation matrix from the inertial frame to the body fixed system is seen to be

$$\begin{aligned} \begin{pmatrix} x \\ y \\ z \end{pmatrix} &= \begin{pmatrix} 1 & 0 & 0 \\ 0 & \cos \Phi & \sin \Phi \\ 0 & -\sin \Phi & \cos \Phi \end{pmatrix} \begin{pmatrix} \cos \Theta & 0 & -\sin \Theta \\ 0 & 1 & 0 \\ \sin \Theta & 0 & \cos \Theta \end{pmatrix} \begin{pmatrix} x_f \\ y_f \\ z_f \end{pmatrix} \\ &= \begin{pmatrix} \cos \Theta & 0 & -\sin \Theta \\ \sin \Theta \sin \Phi & \cos \Phi & \cos \Theta \sin \Phi \\ \sin \Theta \cos \Phi & -\sin \Phi & \cos \Theta \cos \Phi \end{pmatrix} \begin{pmatrix} x_f \\ y_f \\ z_f \end{pmatrix} \end{aligned} \quad (4.10)$$

The components of the gravitational acceleration in the body-fixed system are, therefore,

$$\begin{pmatrix} g_x \\ g_y \\ g_z \end{pmatrix} = \begin{pmatrix} \cos \Theta & 0 & -\sin \Theta \\ \sin \Theta \sin \Phi & \cos \Phi & \cos \Theta \sin \Phi \\ \sin \Theta \cos \Phi & -\sin \Phi & \cos \Theta \cos \Phi \end{pmatrix} \begin{pmatrix} 0 \\ 0 \\ g_0 \end{pmatrix} = g_0 \begin{pmatrix} -\sin \Theta \\ \cos \Theta \sin \Phi \\ \cos \Theta \cos \Phi \end{pmatrix} \quad (4.11)$$

The force equations can thus be written as

$$\begin{pmatrix} X \\ Y \\ Z \end{pmatrix} + mg_0 \begin{pmatrix} -\sin \Theta \\ \cos \Theta \sin \Phi \\ \cos \Theta \cos \Phi \end{pmatrix} = m \begin{pmatrix} \dot{u} + qw - rv \\ \dot{v} + ru - pw \\ \dot{w} + pv - qu \end{pmatrix} \quad (4.12)$$

where (X, Y, Z) are the components of the net aerodynamic and propulsive forces acting on the vehicle, which will be characterized in subsequent sections.

4.1.2 Moment Equations

The vector form of the equation relating the net torque to the rate of change of angular momentum is

$$\vec{G} = \begin{pmatrix} L \\ M \\ N \end{pmatrix} = \int_m (\vec{r} \times \vec{a}) dm \quad (4.13)$$

where (L, M, N) are the components about the (x, y, z) body axes, respectively, of the net aerodynamic and propulsive moments acting on the vehicle. Note that there is no net moment due to the gravitational forces, since the origin of the body-axis system has been chosen at the center of mass of the vehicle. The components of Eq.(4.13) can be written as

$$\begin{aligned} L &= \int_m (y\ddot{z} - z\ddot{y}) dm \\ M &= \int_m (z\ddot{x} - x\ddot{z}) dm \\ N &= \int_m (x\ddot{y} - y\ddot{x}) dm \end{aligned} \quad (4.14)$$

where \ddot{x} , \ddot{y} , and \ddot{z} are the net accelerations in an inertial system instantaneously coincident with the body axis system, as given in Eqs. (4.4).

When Eqs. (4.4) are substituted into Eqs. (4.14), the terms in the resulting integrals are either linear or quadratic in the coordinates. Since the origin of the body-axis system is at the vehicle c.g.,

Eqs. (4.6) apply and the linear terms integrate to zero. The quadratic terms can be expressed in terms of the *moments of inertia*

$$\begin{aligned} I_x &= \int_m (y^2 + z^2) \, dm \\ I_y &= \int_m (z^2 + x^2) \, dm \\ I_z &= \int_m (x^2 + y^2) \, dm \end{aligned} \quad (4.15)$$

and the *product of inertia*

$$I_{xz} = \int_m xz \, dm \quad (4.16)$$

Note that the products of inertia $I_{xy} = I_{yz} = 0$, since the y -axis is perpendicular to the assumed plane of symmetry of the vehicle.

Equations (4.14) can then be written as

$$\begin{aligned} L &= I_x \dot{p} + (I_z - I_y) qr - I_{xz} (pq + \dot{r}) \\ M &= I_y \dot{q} + (I_x - I_z) rp - I_{xz} (p^2 - r^2) \\ N &= I_z \dot{r} + (I_y - I_x) pq - I_{xz} (qr - \dot{p}) \end{aligned} \quad (4.17)$$

Note that if principal axes are used, so that $I_{xz} \equiv 0$, Eqs. (4.17) simplify to

$$\begin{aligned} L &= I_x \dot{p} + (I_z - I_y) qr \\ M &= I_y \dot{q} + (I_x - I_z) rp \\ N &= I_z \dot{r} + (I_y - I_x) pq \end{aligned} \quad (4.18)$$

4.2 Linearized Equations of Motion

The equations developed in the preceding section completely describe the motion of a flight vehicle, subject to the prescribed aerodynamic (and propulsive) forces and moments. These equations are *nonlinear* and *coupled*, however, and generally can be solved only numerically, yielding relatively little insight into the dependence of the stability and controllability of the vehicle on basic aerodynamic parameters of the vehicle.

A great deal, however, can be learned by studying *linear* approximations to these equations. In this approach, we analyze the solutions to the equations describing *small perturbations* about an equilibrium flight condition. The greatest simplification of the equations arises when the equilibrium condition is chosen to correspond to a *longitudinal* equilibrium, in which the velocity and gravity vectors lie in the plane of symmetry of the vehicle; the most common choice corresponds to unaccelerated flight – i.e., to level, unaccelerated flight, or to steady climbing (or descending) flight. Such a linear analysis has been remarkably successful in flight dynamics applications,³ primarily because:

³This statement should be interpreted in the context of the difficulty of applying similar linear analyses to other situations – e.g., to road vehicle dynamics, in which the stability derivatives associated with tire forces are notoriously nonlinear.

1. Over a fairly broad range of flight conditions of practical importance, the aerodynamic forces and moments are well-approximated as linear functions of the state variables; and
2. Normal flight situations correspond to relatively small variations in the state variables; in fact, relatively small disturbances in the state variables can lead to significant accelerations, i.e., to flight of considerable violence, which we normally want to avoid.

Finally, we should emphasize the caveat that these linear analyses are not good approximations in some cases – particularly for spinning or post-stall flight situations.

Thus, we will consider

1. Perturbations from a longitudinal trim condition;
2. Using stability axes;

so we can describe the state variables as

$$\begin{aligned}
 u &= u_0 + u(t), & p &= p(t) \\
 v &= v(t), & q &= q(t) \\
 w &= w(t), & r &= r(t) \\
 \theta &= \Theta_0 + \theta(t), & \Phi &= \phi(t)
 \end{aligned} \tag{4.19}$$

Variables with the subscript $_0$ correspond to the original equilibrium (trim) state. Note that only the axial velocity u and pitch angle θ have non-zero equilibrium values. The trim values of all lateral/directional variables (v , p , r , and Φ) are zero because the initial trim condition corresponds to longitudinal equilibrium; the equilibrium value of w is zero because we are using stability axes; and the equilibrium pitch rate q is assumed zero as we are restricting the equilibrium state to have no normal acceleration.

The equations for the unperturbed initial equilibrium state then reduce to

$$\begin{aligned}
 X_0 - mg_0 \sin \Theta_0 &= 0 \\
 Z_0 + mg_0 \cos \Theta_0 &= 0 \\
 M_0 = L_0 = Y_0 = N_0 &= 0
 \end{aligned} \tag{4.20}$$

and we want to solve linear approximations to the equations

$$\begin{aligned}
 X_0 + \Delta X - mg_0 \sin (\Theta_0 + \theta) &= m (\dot{u} + qw - rv) \\
 Y_0 + \Delta Y + mg_0 \cos (\Theta_0 + \theta) \sin \phi &= m (\dot{v} + r(u_0 + u) - pw) \\
 Z_0 + \Delta Z + mg_0 \cos (\Theta_0 + \theta) \cos \phi &= m (\dot{w} + pv - q(u_0 + u))
 \end{aligned} \tag{4.21}$$

and

$$\begin{aligned}
 \Delta L &= I_x \dot{p} + (I_z - I_y) qr - I_{xz} (pq + \dot{r}) \\
 \Delta M &= I_y \dot{q} + (I_x - I_z) rp + I_{xz} (p^2 - r^2) \\
 \Delta N &= I_z \dot{r} + (I_y - I_x) pq + I_{xz} (qr - \dot{p})
 \end{aligned} \tag{4.22}$$

Since we assume that all perturbation quantities are small, we can approximate

$$\begin{aligned}
 \sin (\Theta_0 + \theta) &\approx \sin \Theta_0 + \theta \cos \Theta_0 \\
 \cos (\Theta_0 + \theta) &\approx \cos \Theta_0 - \theta \sin \Theta_0
 \end{aligned} \tag{4.23}$$

and

$$\begin{aligned}\sin \Phi &= \sin \phi \approx \phi \\ \cos \Phi &= \cos \phi \approx 1\end{aligned}\tag{4.24}$$

Thus, after making these approximations, subtracting the equilibrium equations, and neglecting terms that are quadratic in the small perturbations, the force equations can be written

$$\begin{aligned}\Delta X - mg_0 \cos \Theta_0 \theta &= m\dot{u} \\ \Delta Y + mg_0 \cos \Theta_0 \phi &= m(\dot{v} + u_0 r) \\ \Delta Z - mg_0 \sin \Theta_0 \theta &= m(\dot{w} - u_0 q)\end{aligned}\tag{4.25}$$

and the moment equations can be written

$$\begin{aligned}\Delta L &= I_x \dot{p} - I_{xz} \dot{r} \\ \Delta M &= I_y \dot{q} \\ \Delta N &= I_z \dot{r} - I_{xz} \dot{p}\end{aligned}\tag{4.26}$$

4.3 Representation of Aerodynamic Forces and Moments

The perturbations in aerodynamic forces and moments are functions of both, the perturbations in state variables and control inputs. The most important dependencies can be represented as follows. The dependencies in the equations describing the longitudinal state variables can be written

$$\begin{aligned}\Delta X &= \frac{\partial X}{\partial u} u + \frac{\partial X}{\partial w} w + \frac{\partial X}{\partial \dot{\delta}_e} \delta_e + \frac{\partial X}{\partial \delta_T} \delta_T \\ \Delta Z &= \frac{\partial Z}{\partial u} u + \frac{\partial Z}{\partial w} w + \frac{\partial Z}{\partial \dot{w}} \dot{w} + \frac{\partial Z}{\partial q} q + \frac{\partial Z}{\partial \delta_e} \delta_e + \frac{\partial Z}{\partial \delta_T} \delta_T \\ \Delta M &= \frac{\partial M}{\partial u} u + \frac{\partial M}{\partial w} w + \frac{\partial M}{\partial \dot{w}} \dot{w} + \frac{\partial M}{\partial q} q + \frac{\partial M}{\partial \delta_e} \delta_e + \frac{\partial M}{\partial \delta_T} \delta_T\end{aligned}\tag{4.27}$$

In these equations, the control variables δ_e and δ_T correspond to perturbations from trim in the elevator and thrust (throttle) settings. Note that the Z force and pitching moment M are assumed to depend on both the rate of change of angle of attack \dot{w} and the pitch rate q , but the dependence of the X force on these variables is neglected.

Also, the dependencies in the equations describing the lateral/directional state variables can be written

$$\begin{aligned}\Delta Y &= \frac{\partial Y}{\partial v} v + \frac{\partial Y}{\partial p} p + \frac{\partial Y}{\partial r} r + \frac{\partial Y}{\partial \delta_r} \delta_r \\ \Delta L &= \frac{\partial L}{\partial v} v + \frac{\partial L}{\partial p} p + \frac{\partial L}{\partial r} r + \frac{\partial L}{\partial \delta_r} \delta_r + \frac{\partial L}{\partial \delta_a} \delta_a \\ \Delta N &= \frac{\partial N}{\partial v} v + \frac{\partial N}{\partial p} p + \frac{\partial N}{\partial r} r + \frac{\partial N}{\partial \delta_r} \delta_r + \frac{\partial N}{\partial \delta_a} \delta_a\end{aligned}\tag{4.28}$$

In these equations, the variables δ_r and δ_a represent the perturbations from trim in the rudder and aileron control settings.

Note that the representations in Eqs. (4.27) and (4.28) are completely decoupled. That is, the perturbations in longitudinal forces and moments (ΔX , ΔZ , and ΔM) depend neither on the lateral/directional perturbations (v , p , and r) nor the lateral/directional control inputs (δ_r and δ_a); And the perturbations in lateral/directional forces and moments (ΔY , ΔL , and ΔN) depend neither on the longitudinal perturbations (u , w , \dot{w} , and q) nor the longitudinal control inputs (δ_e and δ_T). This is a good approximation for vehicles with left/right symmetry. This decoupling is *exact* for the dependence of the lateral/directional forces and moments on the longitudinal state variables, since a change in a longitudinal variable, say angle of attack, cannot produce a change in the side force, rolling moment, or yawing moment, for a perfectly symmetric vehicle. The decoupling is only *approximate* for the dependence of the longitudinal forces and moments on the lateral/directional state variables, since a change in a lateral/directional variable, say roll rate, produces no change in axial or vertical force or pitching moment only to within first order for a symmetric vehicle. Consider, for example, the change in lift force due to roll rate. The increased lift on the down-going wing is canceled by the decreased lift on the upgoing wing only to within the linear approximation.

The final form of the dimensional small-perturbation equations is developed by defining the stability derivatives corresponding to force perturbations by dividing them by the vehicle mass, and by defining the stability derivatives corresponding to moment perturbations by dividing them by the corresponding moments of inertia of the vehicle. Thus, we *define*

$$\begin{aligned} X_u &\equiv \frac{1}{m} \frac{\partial X}{\partial u}, & X_w &\equiv \frac{1}{m} \frac{\partial X}{\partial w}, & \dots & X_{\delta_T} &\equiv \frac{1}{m} \frac{\partial X}{\partial \delta_T}; \\ Y_v &\equiv \frac{1}{m} \frac{\partial Y}{\partial v}, & Y_p &\equiv \frac{1}{m} \frac{\partial Y}{\partial p}, & \dots & Y_{\delta_r} &\equiv \frac{1}{m} \frac{\partial Y}{\partial \delta_r}; \\ Z_u &\equiv \frac{1}{m} \frac{\partial Z}{\partial u}, & Z_w &\equiv \frac{1}{m} \frac{\partial Z}{\partial w}, & \dots & Z_{\delta_T} &\equiv \frac{1}{m} \frac{\partial Z}{\partial \delta_T}; \end{aligned} \quad (4.29)$$

and

$$\begin{aligned} L_v &\equiv \frac{1}{I_x} \frac{\partial L}{\partial v}, & L_p &\equiv \frac{1}{I_x} \frac{\partial L}{\partial p}, & \dots & L_{\delta_a} &\equiv \frac{1}{I_x} \frac{\partial L}{\partial \delta_a}; \\ M_u &\equiv \frac{1}{I_y} \frac{\partial M}{\partial u}, & M_w &\equiv \frac{1}{I_y} \frac{\partial M}{\partial w}, & \dots & M_{\delta_T} &\equiv \frac{1}{I_y} \frac{\partial M}{\partial \delta_T}; \\ N_v &\equiv \frac{1}{I_z} \frac{\partial N}{\partial v}, & N_p &\equiv \frac{1}{I_z} \frac{\partial N}{\partial p}, & \dots & N_{\delta_a} &\equiv \frac{1}{I_z} \frac{\partial N}{\partial \delta_a}. \end{aligned} \quad (4.30)$$

It is important to emphasize that the quantities defined by these equations are not to be interpreted simply as (the usual mathematical notation for) partial derivatives but, rather, are the expected partial derivatives divided by the vehicle mass or appropriate moment of inertia.

When these definitions are substituted back into Eqs. (4.27) and (4.28), and these representations are then used in Eqs. (4.25) and (4.26), we arrive at the *small-disturbance equations for longitudinal motions*:

$$\begin{aligned} &\left[\frac{d}{dt} - X_u \right] u + g_0 \cos \Theta_0 \theta - X_w w = X_{\delta_e} \delta_e + X_{\delta_T} \delta_T \\ -Z_u u + \left[(1 - Z_{\dot{w}}) \frac{d}{dt} - Z_w \right] w - [u_0 + Z_q] q + g_0 \sin \Theta_0 \theta &= Z_{\delta_e} \delta_e + Z_{\delta_T} \delta_T \\ -M_u u - \left[M_{\dot{w}} \frac{d}{dt} + M_w \right] w + \left[\frac{d}{dt} - M_q \right] q &= M_{\delta_e} \delta_e + M_{\delta_T} \delta_T \end{aligned} \quad (4.31)$$

and the *small-disturbance equations for lateral/directional motions*:

$$\begin{aligned} \left[\frac{d}{dt} - Y_v \right] v - Y_p p + [u_0 - Y_r] r - g_0 \cos \Theta_0 \phi &= Y_{\delta_r} \delta_r \\ -L_v v + \left[\frac{d}{dt} - L_p \right] p - \left[\frac{I_{xz}}{I_x} \frac{d}{dt} + L_r \right] r &= L_{\delta_r} \delta_r + L_{\delta_a} \delta_a \\ -N_v v - \left[\frac{I_{xz}}{I_z} \frac{d}{dt} + N_p \right] p + \left[\frac{d}{dt} - N_r \right] r &= N_{\delta_r} \delta_r + N_{\delta_a} \delta_a \end{aligned} \quad (4.32)$$

4.3.1 Longitudinal Stability Derivatives

In order to solve the equations describing longitudinal vehicle motions, we need to be able to evaluate all the coefficients appearing in Eqs. (4.31). This means we need to be able to provide estimates for the derivatives of X , Z , and M with respect to the relevant independent variables u , w , \dot{w} , and q . These stability derivatives usually are expressed in terms of dimensionless aerodynamic coefficient derivatives. For example, we can express the stability derivative X_u as

$$X_u \equiv \frac{1}{m} \frac{\partial X}{\partial u} = \frac{1}{m} \frac{\partial}{\partial u} [QS\mathbf{C}_X] = \frac{QS}{mu_0} [2\mathbf{C}_{X0} + \mathbf{C}_{Xu}] \quad (4.33)$$

where

$$\mathbf{C}_{Xu} \equiv \frac{\partial \mathbf{C}_X}{\partial (u/u_0)} \quad (4.34)$$

is the derivative of the dimensionless X -force coefficient with respect to the dimensionless velocity u/u_0 . Note that the first term in the final expression of Eq. (4.33) arises because the dynamic pressure Q is, itself, a function of the flight velocity $u_0 + u$. Similar expressions can be developed for all the required derivatives.

Derivatives with respect to vertical velocity perturbations w are related to aerodynamic derivatives with respect to angle of attack α , since

$$\alpha = \tan^{-1} \left(\frac{w}{u} \right) \approx \frac{w}{u_0} \quad (4.35)$$

Then, for example

$$Z_w \equiv \frac{1}{m} \frac{\partial Z}{\partial w} = \frac{1}{m} \frac{\partial}{\partial (u_0 \alpha)} [QS\mathbf{C}_Z] = \frac{QS}{mu_0} \mathbf{C}_{Z\alpha} \quad (4.36)$$

Derivatives with respect to pitch rate q are related to aerodynamic derivatives with respect to dimensionless pitch rate $\hat{q} \equiv \frac{\bar{c}q}{2u_0}$. Thus, for example

$$M_q \equiv \frac{1}{I_y} \frac{\partial M}{\partial q} = \frac{1}{I_y} \frac{\partial}{\partial \left(\frac{2u_0 \hat{q}}{\bar{c}} \right)} [QS\bar{c}\mathbf{C}_m] = \frac{QS\bar{c}^2}{2I_y u_0} \mathbf{C}_{mq} \quad (4.37)$$

where

$$\mathbf{C}_{mq} \equiv \frac{\partial \mathbf{C}_m}{\partial \hat{q}} \quad (4.38)$$

is the derivative of the dimensionless pitching moment coefficient with respect to the dimensionless pitch rate \hat{q} . In a similar way, dimensionless derivatives with respect to rate of change of angle of attack $\dot{\alpha}$ are expressed in terms of the dimensionless rate of change $\hat{\dot{\alpha}} = \frac{\bar{c}\dot{\alpha}}{2u_0}$.

Variable	X	Z	M
u	$X_u = \frac{QS}{mu_0} [2\mathbf{C}_{X0} + \mathbf{C}_{Xu}]$	$Z_u = \frac{QS}{mu_0} [2\mathbf{C}_{Z0} + \mathbf{C}_{Zu}]$	$M_u = \frac{QS\bar{c}}{I_y u_0} \mathbf{C}_{mu}$
w	$X_w = \frac{QS}{mu_0} \mathbf{C}_{X\alpha}$	$Z_w = \frac{QS}{mu_0} \mathbf{C}_{Z\alpha}$	$M_w = \frac{QS\bar{c}}{I_y u_0} \mathbf{C}_{m\alpha}$
\dot{w}	$X_{\dot{w}} = 0$	$Z_{\dot{w}} = \frac{QS\bar{c}}{2mu_0^2} \mathbf{C}_{Z\dot{\alpha}}$	$M_{\dot{w}} = \frac{QS\bar{c}^2}{2I_y u_0^2} \mathbf{C}_{m\dot{\alpha}}$
q	$X_q = 0$	$Z_q = \frac{QS\bar{c}}{2mu_0} \mathbf{C}_{Zq}$	$M_q = \frac{QS\bar{c}^2}{2I_y u_0} \mathbf{C}_{mq}$

Table 4.1: Relation of dimensional stability derivatives for longitudinal motions to dimensionless derivatives of aerodynamic coefficients.

Expressions for all the dimensional stability derivatives appearing in Eqs. (4.31) in terms of the dimensionless aerodynamic coefficient derivatives are summarized in Table 4.1.

Aerodynamic Derivatives

In this section we relate the dimensionless derivatives of the preceding section to the usual aerodynamic derivatives, and provide simple formulas for estimating them. It is natural to express the axial and normal force coefficients in terms of the lift and drag coefficients, but we must take into account the fact that perturbations in angle of attack will rotate the lift and drag vectors with respect to the body axes. Here, consistent with Eq. (4.35), we define the angle of attack as the angle between the instantaneous vehicle velocity vector and the x -axis, and also assume that the propulsive thrust is aligned with the x -axis. Thus, as seen in Fig. 4.3, we have to within terms linear in angle of attack

$$\begin{aligned} \mathbf{C}_X &= \mathbf{C}_T - \mathbf{C}_D \cos \alpha + \mathbf{C}_L \sin \alpha \approx \mathbf{C}_T - \mathbf{C}_D + \mathbf{C}_L \alpha \\ \mathbf{C}_Z &= -\mathbf{C}_D \sin \alpha - \mathbf{C}_L \cos \alpha \approx -\mathbf{C}_D \alpha - \mathbf{C}_L \end{aligned} \quad (4.39)$$

Here the thrust coefficient

$$\mathbf{C}_T \equiv \frac{T}{QS} \quad (4.40)$$

where T is the net propulsive thrust, assumed to be aligned with the x -axis of the body-fixed system. Since all the dimensionless coefficients in Eqs. (4.39) are normalized by the same quantity QS , the representations of forces and force coefficients are equivalent.

Speed Derivatives

We first consider the derivatives with respect to vehicle speed u . The derivative

$$\mathbf{C}_{Xu} = \mathbf{C}_{Tu} - \mathbf{C}_{Du} \quad (4.41)$$

represents the *speed damping*, and

$$\mathbf{C}_{Du} = \mathbf{M} \frac{\partial \mathbf{C}_D}{\partial \mathbf{M}} \quad (4.42)$$

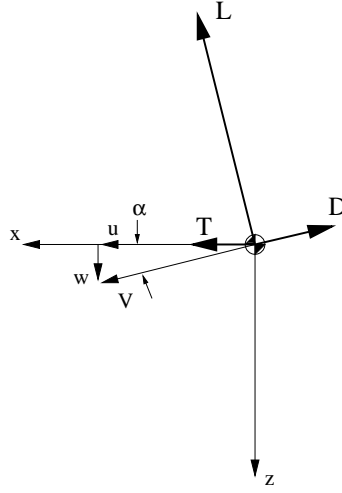


Figure 4.3: Orientation of body axes with respect to instantaneous vehicle velocity, illustrating relation between force components in body axes and lift and drag forces.

represents the contribution of compressibility effects to this derivative.

The contribution of the derivative \mathbf{C}_{T_u} must be estimated separately for the special cases of constant thrust (appropriate for jet-powered aircraft or for a power-off glide), or constant power (appropriate for piston-powered aircraft with constant-speed propellers). For the constant thrust case,

$$\mathbf{C}_{T_u} = \frac{\partial}{\partial(u/u_0)} \left(\frac{T}{QS} \right) = -2\mathbf{C}_{T_0} \quad (4.43)$$

And for the constant power case,

$$\mathbf{C}_{T_u} = \frac{\partial}{\partial(u/u_0)} \left(\frac{P}{QS u} \right) = -3\mathbf{C}_{T_0} \quad (4.44)$$

The equilibrium force equations shown in Eqs. (4.20) can be combined to express the equilibrium thrust coefficient as

$$\mathbf{C}_{T_0} = \mathbf{C}_{D_0} + \mathbf{C}_{L_0} \tan \Theta_0 \quad (4.45)$$

which then gives

$$\mathbf{C}_{X_u} = \begin{cases} -2\mathbf{C}_{D_0} - 2\mathbf{C}_{L_0} \tan \Theta_0 - \mathbf{M}\mathbf{C}_{D_M} & \text{for constant thrust} \\ -3\mathbf{C}_{D_0} - 3\mathbf{C}_{L_0} \tan \Theta_0 - \mathbf{M}\mathbf{C}_{D_M} & \text{for constant power} \end{cases} \quad (4.46)$$

And, when these expressions are substituted into the equation for the dimensional stability derivative from the preceding section, we have

$$X_u = \begin{cases} -\frac{QS}{mu_0} [2\mathbf{C}_{D_0} + \mathbf{M}\mathbf{C}_{D_M}] & \text{for constant thrust} \\ -\frac{QS}{mu_0} [3\mathbf{C}_{D_0} + \mathbf{C}_{L_0} \tan \Theta_0 + \mathbf{M}\mathbf{C}_{D_M}] & \text{for constant power} \end{cases} \quad (4.47)$$

The derivative of the normal force coefficient \mathbf{C}_Z with respect to vehicle speed u is simply

$$\mathbf{C}_{Z_u} = -\mathbf{C}_{L_u} \quad (4.48)$$

since the drag coefficient contribution vanishes when evaluated at the initial trim condition, where $\alpha = 0$. The dependence of lift coefficient on speed arises due to compressibility and aeroelastic effects. We will neglect aeroelastic effects, but the effect of compressibility can be characterized as

$$\mathbf{C}_{Lu} = \mathbf{M} \frac{\partial \mathbf{C}_L}{\partial \mathbf{M}} \quad (4.49)$$

where \mathbf{M} is the flight Mach number. The Prandtl-Glauert similarity law for subsonic flow gives

$$\mathbf{C}_L = \frac{\mathbf{C}_L|_{\mathbf{M}=0}}{\sqrt{1-\mathbf{M}^2}} \quad (4.50)$$

which can be used to show that

$$\frac{\partial \mathbf{C}_L}{\partial \mathbf{M}} = \frac{\mathbf{M}}{1-\mathbf{M}^2} \mathbf{C}_{L0} \quad (4.51)$$

whence

$$\mathbf{C}_{Zu} = -\frac{\mathbf{M}^2}{1-\mathbf{M}^2} \mathbf{C}_{L0} \quad (4.52)$$

Use of the corresponding form of the Prandtl-Glauert rule for supersonic flow results in exactly the same formula. We then have for the dimensional stability derivative

$$Z_u = -\frac{QS}{mu_0} \left[2\mathbf{C}_{L0} + \frac{\mathbf{M}^2}{1-\mathbf{M}^2} \mathbf{C}_{L0} \right] \quad (4.53)$$

Finally, the change in pitching moment coefficient \mathbf{C}_m with speed u is generally due to effects of compressibility and aeroelastic deformation. The latter will again be neglected, so we have only the compressibility effect, which can be represented as

$$\mathbf{C}_{mu} = \mathbf{M} \frac{\partial \mathbf{C}_m}{\partial \mathbf{M}} \quad (4.54)$$

so we have

$$M_u = \frac{QS\bar{c}}{I_y u_0} \mathbf{M} \mathbf{C}_{m\mathbf{M}} \quad (4.55)$$

Angle-of-Attack Derivatives

As mentioned earlier, the derivatives with respect to vertical velocity w are expressed in terms of derivatives with respect to angle of attack α . Since from Eq. (4.39) we have

$$\mathbf{C}_X = \mathbf{C}_T - \mathbf{C}_D + \mathbf{C}_L \alpha \quad (4.56)$$

we have

$$\mathbf{C}_{X\alpha} = \mathbf{C}_{T\alpha} - \mathbf{C}_{D\alpha} + \mathbf{C}_{L\alpha} \alpha + \mathbf{C}_L = -\mathbf{C}_{D\alpha} + \mathbf{C}_{L0} \quad (4.57)$$

since we assume the propulsive thrust is independent of the angle of attack, i.e., $\mathbf{C}_{T\alpha} = 0$. Using the parabolic approximation for the drag polar

$$\mathbf{C}_D = \mathbf{C}_{Dp} + \frac{\mathbf{C}_L^2}{\pi e \mathbf{AR}} \quad (4.58)$$

we have

$$\mathbf{C}_{D\alpha} = \frac{2\mathbf{C}_L}{\pi e \mathbf{AR}} \mathbf{C}_{L\alpha} \quad (4.59)$$

and

$$X_w = \frac{QS}{mu_0} \left(\mathbf{C}_{L0} - \frac{2\mathbf{C}_{L0}}{\pi e \mathbf{AR}} \mathbf{C}_{L\alpha} \right) \quad (4.60)$$

Similarly, for the z -force coefficient Eq. (4.39) gives

$$\mathbf{C}_Z = -\mathbf{C}_{D0} - \mathbf{C}_L \quad (4.61)$$

whence

$$\mathbf{C}_{Z\alpha} = -\mathbf{C}_{D0} - \mathbf{C}_{L\alpha} \quad (4.62)$$

so

$$Z_w = -\frac{QS}{mu_0} (\mathbf{C}_{D0} + \mathbf{C}_{L\alpha}) \quad (4.63)$$

Finally, the dimensional derivative of pitching moment with respect to vertical velocity w is given by

$$M_w = \frac{QS\bar{c}}{I_y u_0} \mathbf{C}_{m\alpha} \quad (4.64)$$

Pitch-rate Derivatives

The pitch rate derivatives have already been discussed in our review of static longitudinal stability. As seen there, the principal contribution is from the horizontal tail and is given by

$$\mathbf{C}_{m,q} = -2\eta \frac{\ell_t}{c} V_H a_t \quad (4.65)$$

and

$$\mathbf{C}_{L,q} = 2\eta V_H a_t \quad (4.66)$$

so

$$\mathbf{C}_{Z,q} = -\mathbf{C}_{L,q} = -2\eta V_H a_t \quad (4.67)$$

The derivative $\mathbf{C}_{X,q}$ is usually assumed to be negligibly small.

Angle-of-attack Rate Derivatives

The derivatives with respect to *rate of change* of angle of attack $\dot{\alpha}$ arise primarily from the time lag associated with wing downwash affecting the horizontal tail. This affects the lift force on the horizontal tail and the corresponding pitching moment; the effect on vehicle drag usually is neglected.

The wing downwash is associated with the vorticity trailing behind the wing and, since vorticity is convected with the local fluid velocity, the time lag for vorticity to convect from the wing to the tail is approximately

$$\Delta t = \frac{\ell_t}{u_0}$$

The instantaneous angle of attack seen by the horizontal tail is therefore

$$\alpha_t = \alpha + i_t - \varepsilon = \alpha + i_t - \left[\varepsilon_0 + \frac{d\varepsilon}{d\alpha} (\alpha - \dot{\alpha}\Delta t) \right] \quad (4.68)$$

so

$$\frac{d\alpha_t}{d\dot{\alpha}} = \frac{d\varepsilon}{d\alpha} \Delta t = \frac{\ell_t}{u_0} \frac{d\varepsilon}{d\alpha} \quad (4.69)$$

The rate of change of tail lift with $\dot{\alpha}$ is then seen to be

$$\frac{dL_t}{d\dot{\alpha}} = Q_t S_t a_t \frac{\ell_t}{u_0} \frac{d\varepsilon}{d\alpha} = \eta Q S_t a_t \frac{\ell_t}{u_0} \frac{d\varepsilon}{d\alpha} \quad (4.70)$$

so the change in normal force coefficient with respect to dimensionless $\dot{\alpha}$ is

$$\mathbf{C}_{Z\dot{\alpha}} \equiv \frac{\partial \mathbf{C}_Z}{\partial \frac{\varepsilon \dot{\alpha}}{2u_0}} = -2\eta V_H a_t \frac{d\varepsilon}{d\alpha} \quad (4.71)$$

The corresponding change in pitching moment is

$$\frac{dM_{cg}}{d\dot{\alpha}} = -\ell_t \frac{dL_t}{d\dot{\alpha}} = -\eta Q S_t a_t \frac{\ell_t^2}{u_0} \frac{d\varepsilon}{d\alpha} \quad (4.72)$$

so the change in pitching moment coefficient with respect to dimensionless $\dot{\alpha}$ is

$$\mathbf{C}_{m\dot{\alpha}} \equiv \frac{\partial \mathbf{C}_m}{\partial \frac{\varepsilon \dot{\alpha}}{2u_0}} = -2\eta \frac{\ell_t}{c} V_H a_t \frac{d\varepsilon}{d\alpha} = \frac{\ell_t}{c} \mathbf{C}_{Z\dot{\alpha}} \quad (4.73)$$

4.3.2 Lateral/Directional Stability Derivatives

In order to solve the equations describing lateral/directional vehicle motions, we need to be able to evaluate all the coefficients appearing in Eqs. (4.32). This means we need to be able to provide estimates for the derivatives of Y , L , and N with respect to the relevant independent variables v , p , and r . As for the longitudinal case, these stability derivatives usually are expressed in terms of dimensionless aerodynamic coefficient derivatives.

Derivatives with respect to lateral velocity perturbations v are related to aerodynamic derivatives with respect to angle of sideslip β , since

$$\beta = \tan^{-1} \left(\frac{v}{V} \right) \approx \frac{v}{u_0} \quad (4.74)$$

For example, we can express the stability derivative Y_v as

$$Y_v \equiv \frac{1}{m} \frac{\partial Y}{\partial (u_0 \beta)} = \frac{1}{m u_0} \frac{\partial}{\partial \beta} [Q S \mathbf{C}_y] = \frac{Q S}{m u_0} \mathbf{C}_{y\beta} \quad (4.75)$$

where

$$\mathbf{C}_{y\beta} \equiv \frac{\partial \mathbf{C}_y}{\partial \beta} \quad (4.76)$$

is the derivative of the dimensionless Y -force coefficient with respect to the sideslip angle $\beta = v/u_0$. Similar expressions can be developed for all the required derivatives.

Derivatives with respect to roll rate p and yaw rate r are related to aerodynamic derivatives with respect to the corresponding dimensionless rate, either $\hat{p} \equiv \frac{pb}{2u_0}$, or $\hat{r} \equiv \frac{rb}{2u_0}$. Thus, for example, the roll damping derivative

$$L_p \equiv \frac{1}{I_x} \frac{\partial L}{\partial p} = \frac{1}{I_x} \frac{\partial}{\partial \left(\frac{2u_0 \hat{p}}{b} \right)} [Q S b \mathbf{C}_l] = \frac{Q S b^2}{2 I_x u_0} \mathbf{C}_{l_p} \quad (4.77)$$

Variable	Y	L	N
v	$Y_v = \frac{QS}{mu_0} \mathbf{C}_{y\beta}$	$L_v = \frac{Q Sb}{I_x u_0} \mathbf{C}_{l\beta}$	$N_v = \frac{Q Sb}{I_z u_0} \mathbf{C}_{n\beta}$
p	$Y_p = \frac{Q Sb}{2mu_0} \mathbf{C}_{yp}$	$L_p = \frac{Q Sb^2}{2I_x u_0} \mathbf{C}_{lp}$	$N_p = \frac{Q Sb^2}{2I_z u_0} \mathbf{C}_{np}$
r	$Y_r = \frac{Q Sb}{2mu_0} \mathbf{C}_{yr}$	$L_r = \frac{Q Sb^2}{2I_x u_0} \mathbf{C}_{lr}$	$N_r = \frac{Q Sb^2}{2I_z u_0} \mathbf{C}_{nr}$

Table 4.2: Relation of dimensional stability derivatives for lateral/directional motions to dimensionless derivatives of aerodynamic coefficients.

where

$$\mathbf{C}_{lp} \equiv \frac{\partial \mathbf{C}_l}{\partial \hat{p}} \quad (4.78)$$

is the derivative of the dimensionless rolling moment coefficient with respect to the dimensionless roll rate \hat{p} .⁴

Expressions for all the dimensional stability derivatives appearing in Eqs. (4.32) in terms of the dimensionless aerodynamic coefficient derivatives are summarized in Table 4.2.

Sideslip Derivatives

The side force due to sideslip is due primarily to the side force (or “lift”) produced by the vertical tail, which can be expressed as

$$Y_v = -Q_v S_v \frac{\partial \mathbf{C}_{L_v}}{\partial \alpha_v} \alpha_v \quad (4.79)$$

where the minus sign is required because we define the angle of attack as

$$\alpha_v = \beta + \sigma \quad (4.80)$$

where positive $\beta = \sin^{-1}(v/V)$ corresponds to positive v . The angle σ is the sidewash angle describing the distortion in angle of attack at the vertical tail due to interference effects from the wing and fuselage. The sidewash angle σ is for the vertical tail what the downwash angle ε is for the horizontal tail.⁵

The side force coefficient can then be expressed as

$$\mathbf{C}_y \equiv \frac{Y}{QS} = -\frac{Q_v S_v}{Q S} \frac{\partial \mathbf{C}_{L_v}}{\partial \alpha_v} (\beta + \sigma) \quad (4.81)$$

whence

$$\mathbf{C}_{y\beta} \equiv \frac{\partial \mathbf{C}_y}{\partial \beta} = -\eta_v \frac{S_v}{S} a_v \left(1 + \frac{d\sigma}{d\beta} \right) \quad (4.82)$$

⁴Note that the lateral and directional rates are nondimensionalized using the time scale $b/(2u_0)$ – i.e., the span dimension is used instead of the mean aerodynamic chord which appears in the corresponding quantities for longitudinal motions.

⁵Note, however, that the sidewash angle is defined as having the opposite sign from the downwash angle. This is because the sidewash angle can easily *augment* the sideslip angle at the vertical tail, while the induced downwash at the horizontal tail always reduces the effective angle of attack.

where

$$\eta_v = \frac{Q_v}{Q} \quad (4.83)$$

is the *vertical tail efficiency factor*.

The yawing moment due to side slip is called the *weathercock stability* derivative, and is caused by both, the vertical tail side force acting through the moment arm ℓ_v and the destabilizing yawing moment produced by the fuselage. This latter effect is analogous to the destabilizing contribution of the fuselage to the pitch stiffness $\mathbf{C}_{m\alpha}$, and can be estimated from slender-body theory to be

$$\mathbf{C}_{n\beta})_{fuse} = -2\frac{\mathcal{V}}{Sb} \quad (4.84)$$

where \mathcal{V} is the volume of the equivalent fuselage – based on fuselage height (rather than width, as for the pitch stiffness). The yawing moment contribution due to the side force acting on the vertical tail is

$$N_v = -\ell_v Y_v$$

so the corresponding contribution of the vertical tail to the weathercock stability is

$$\mathbf{C}_{n\beta})_V = \eta_v V_v a_v \left(1 + \frac{d\sigma}{d\beta}\right) \quad (4.85)$$

where

$$V_v = \frac{\ell_v S_v}{bS} \quad (4.86)$$

is the *tail volume ratio* for the vertical tail.

The sum of vertical tail and fuselage contributions to weathercock stability is then

$$\mathbf{C}_{n\beta} = \eta_v V_v a_v \left(1 + \frac{d\sigma}{d\beta}\right) - 2\frac{\mathcal{V}}{Sb} \quad (4.87)$$

Note that a positive value of $\mathbf{C}_{n\beta}$ corresponds to stability, i.e., to the tendency for the vehicle to turn into the relative wind. The first term on the right hand side of Eq. (4.87), that due to the vertical tail, is stabilizing, while the second term, due to the fuselage, is destabilizing. In fact, providing adequate weathercock stability is the principal role of the vertical tail.

The final sideslip derivative describes the effect of sideslip on the rolling moment. The derivative $\mathbf{C}_{l\beta}$ is called the *dihedral effect*, and is one of the most important parameters for lateral/directional stability and handling qualities. A stable dihedral effect causes the vehicle to roll away from the sideslip, preventing the vehicle from “falling off its lift vector.” This requires a negative value of $\mathbf{C}_{l\beta}$.

The dihedral effect has contributions from: (1) geometric dihedral; (2) wing sweep; (3) the vertical tail; and (4) wing-fuselage interaction. The contribution from geometric dihedral can be seen from the sketch in Fig. 4.4. There it is seen that the effect of sideslip is to increase the velocity normal to the plane of the right wing, and to decrease the velocity normal to the plane of the left wing, by the amount $u_0\beta \sin \Gamma$, where Γ is the geometric angle of dihedral. Thus, the effective angles of attack of the right and left wings are increased and decreased, respectively, by

$$\Delta\alpha = \frac{u_0\beta \sin \Gamma}{u_0} = \beta \sin \Gamma \quad (4.88)$$

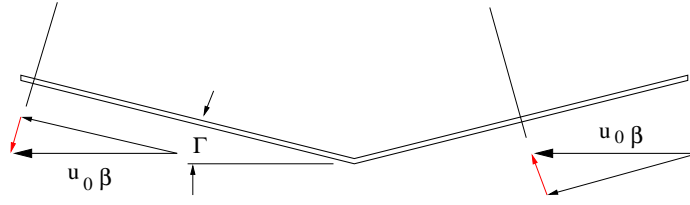


Figure 4.4: Effect of geometric dihedral angle Γ on angle of attack of the left and right wing panels. View is from behind the wing, i.e., looking along the positive x -axis.

Since the change in angle of attack on the right and left wings is of opposite sign, the corresponding change in lift on the two wings produces a rolling moment. The corresponding change in rolling moment coefficient is given by

$$\Delta C_l = \frac{\Delta L}{Q S b} = -\frac{1}{2} \left(a_w (\beta \sin \Gamma) \frac{\bar{y}}{b} + a_w (-\beta \sin \Gamma) \frac{-\bar{y}}{b} \right) = -a_w \sin \Gamma \frac{\bar{y}}{b} \beta \quad (4.89)$$

where \bar{y} is the distance from the c.g. (symmetry plane) to the center of lift for each wing panel.

For an elliptic spanwise load distribution (see Eq. (4.142)), the centroid of lift on the right wing is located at

$$\bar{y} = \frac{4}{3\pi} \frac{b}{2} \quad (4.90)$$

so, combining this result with Eq. (4.89) we have for a wing with an elliptic spanwise loading

$$C_{l\beta} = -\frac{2}{3\pi} a_w \sin \Gamma \quad (4.91)$$

The contribution of wing sweep to dihedral effect arises from the change in effective dynamic pressure on the right and left wing panels due to sideslip, as is illustrated in the sketch in Fig. 4.5. According to simple sweep theory, it is only the components of velocity in the plane normal to the quarter-chord sweep line that contribute to the forces on the wing, so the lift on the each of the wing panels can be expressed as

$$\begin{aligned} (\text{Lift})_R &= C_L \frac{S}{2} Q \cos^2 (\Lambda_{c/4} - \beta) \\ (\text{Lift})_L &= C_L \frac{S}{2} Q \cos^2 (\Lambda_{c/4} + \beta) \end{aligned} \quad (4.92)$$

The net rolling moment coefficient resulting from this lift is then

$$C_l = \frac{C_L \bar{y}}{2} \frac{\bar{y}}{b} [\cos^2 (\Lambda_{c/4} + \beta) - \cos^2 (\Lambda_{c/4} - \beta)] \approx -C_L \frac{\bar{y}}{b} \sin (2\Lambda_{c/4}) \beta \quad (4.93)$$

so the contribution of sweep to dihedral stability is

$$C_{l\beta} = -C_L \frac{\bar{y}}{b} \sin (2\Lambda_{c/4}) \quad (4.94)$$

Using Eq. (4.90), we have the expression specialized to the case of an elliptic spanwise loading:

$$C_{l\beta} = -\frac{2}{3\pi} C_L \sin (2\Lambda_{c/4}) \quad (4.95)$$

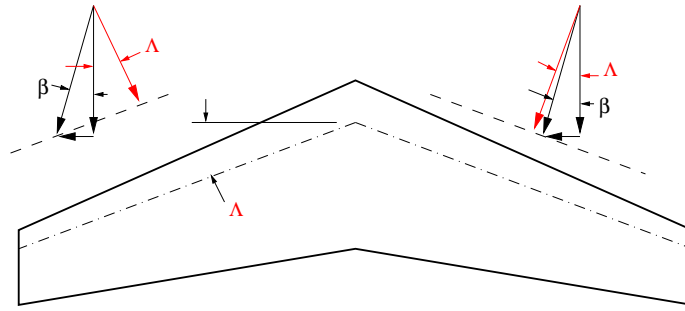


Figure 4.5: Effect of wing sweep dihedral effect. Sideslip increases the effective dynamic pressure on the right wing panel, and decreases it by the same amount on the left wing panel.

Note that the contribution of sweep to dihedral effect is proportional to wing lift coefficient (so it will be more significant at low speeds), and is stabilizing when the wing is swept back.

The contribution of the vertical tail to dihedral effect arises from the rolling moment generated by the side force on the tail. Thus, we have

$$\mathbf{C}_{l\beta} = \frac{z'_v}{b} \mathbf{C}_{y\beta} \quad (4.96)$$

where z'_v is the distance of the vertical tail aerodynamic center above the vehicle center of mass. Using Eq. (4.82), this can be written

$$\mathbf{C}_{l\beta} = -\eta_v \left(\frac{z'_v S_v}{bS} \right) a_v \left(1 + \frac{d\sigma}{d\beta} \right) \quad (4.97)$$

At low angles of attack the contribution of the vertical tail to dihedral effect usually is stabilizing. But, at high angles of attack, z'_v can become negative, in which case the contribution is de-stabilizing.

The contribution to dihedral effect from wing-fuselage interference will be described only qualitatively. The effect arises from the local changes in wing angle of attack due to the flow past the fuselage as sketched in Fig. 4.6. As indicated in the figure, for a low-wing configuration the presence of the fuselage has the effect of locally decreasing the angle of attack of the right wing in the vicinity of the fuselage, and increasing the corresponding angles of attack of the left wing, resulting in an unstable (positive) contribution to $\mathbf{C}_{l\beta}$. For a high-wing configuration, the perturbations in angle of attack are reversed, so the interference effect results in a stable (negative) contribution to $\mathbf{C}_{l\beta}$.

As a result of this wing-fuselage interaction, all other things being equal, a high-wing configuration needs less geometric dihedral than a low-wing one. This effect can be seen by comparing the geometric dihedral angle of a high-wing aircraft with a similar vehicle having a low-wing configuration. For example, the high-wing Lockheed C-5A actually has negative dihedral (or anhedral), while the low-wing Boeing 747 has about 5 degrees of dihedral; see Fig. 4.7.

Finally, it is interesting to consider the dihedral stability of the first powered airplane, the Wright Flyer; a three-view drawing is shown in Fig. 4.8. The Wright Flyer has virtually no fuselage (and, in any event, the biplane configuration of the wings is nearly symmetric with respect to all the bracing, etc.), so there is no wing-fuselage interference contribution to $\mathbf{C}_{l\beta}$. Also, the wing is unswept, so there is no sweep contribution. In fact, the wings have a slight *negative* dihedral, so the craft has a net unstable dihedral effect. The Wright brothers did not consider stability a necessary property for

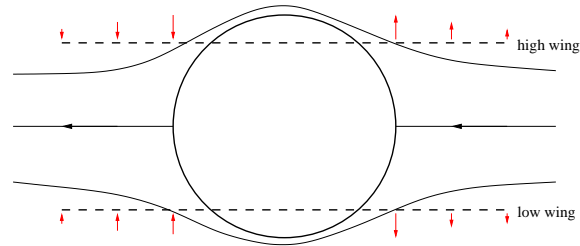


Figure 4.6: Effect of wing-fuselage interference on dihedral effect; figure corresponds to positive sideslip with vehicle viewed from behind. The presence of the fuselage alters the flow due to sideslip locally in the vicinity of the wing. Note that the resulting perturbations in angle of attack for a high-wing configuration are opposite in sign to those for a low-wing configuration, with this phenomenon contributing to stabilizing dihedral effect for the high-wing configuration.



(a) Boeing 747



(b) Lockheed C-5A

Figure 4.7: Illustration of effect of wing-fuselage interference on dihedral effect. The Boeing 747 and Lockheed C-5A have wings with nearly the same sweep angle, but the low-wing 747 requires significantly more geometric dihedral than the high-wing C-5A. Note: the (smaller) high-wing C-130 in the foreground of the photograph on the right requires less negative dihedral (anhedral) than the C-5A because it has an un-swept wing.

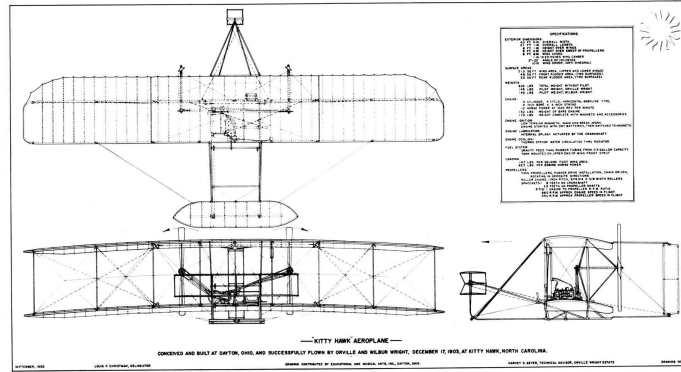


Figure 4.8: Three-view drawing of the Wright Flyer. Note the negative geometric dihedral which, in the absence of other significant contributions to dihedral effect, will almost certainly result in an unstable spiral mode.

a flight vehicle; they started out as bicycle mechanics, and knew that almost anyone could learn to ride an unstable bicycle, so they spent much of their time in early experiments learning how to fly unstable aircraft. Recent re-enactments of Wright Flyer flights, in connection with the centennial celebrations in 2003 of the Wright brothers' first flight, have confirmed the difficulty in learning to fly a vehicle having an unstable dihedral effect!

Derivatives with Respect to Yaw Rate

The stability derivative describing the side force due to yaw rate is

$$Y_r \equiv \frac{1}{m} \frac{\partial Y}{\partial r} = \frac{Q S b}{2 m u_0} C_{y_r} \quad (4.98)$$

where

$$C_{y_r} \equiv \frac{\partial C_y}{\partial \hat{r}} \quad (4.99)$$

and $\hat{r} = rb/(2u_0)$ is the dimensionless yaw rate. The side force due to yaw rate arises primarily from the force on the vertical tail; thus the derivative C_{y_r} is analogous to the longitudinal derivative C_{Z_q} . The change in angle of attack of the vertical tail due to yaw rate is

$$\Delta \alpha_v = \frac{r \ell_v}{u_0} = 2 \frac{\ell_v}{b} \hat{r} \quad (4.100)$$

so the change in side force is

$$\Delta Y = 2 Q_v S_v a_v \frac{\ell_v}{b} \hat{r} \quad (4.101)$$

and the corresponding value of the coefficient derivative is

$$C_{y_r} = 2 \eta_v V_v a_v \quad (4.102)$$

Both the wing and the vertical tail contribute to the rolling moment due to yaw rate. The vertical tail contribution is due to the side force acting through the moment arm z'_v , the distance the vertical

tail aerodynamic center is above the vehicle center of mass. Thus,

$$\mathbf{C}_{lr})_V = \frac{z'_v}{b} \mathbf{C}_{y_r} = 2\eta_v \frac{z'_v}{b} V_v a_v \quad (4.103)$$

The contribution of the wing arises because, as a result of the yaw rate the effective velocity of the left wing is increased, and that of the right wing is decreased (for a positive yaw rate r). This effect increases the lift on the left wing, and decreases it on the right wing. The effect is proportional to the equilibrium lift coefficient and, for an elliptical spanwise loading simple strip theory gives (see Exercise 2)

$$(\mathbf{C}_{lr})_{\text{wing}} = \frac{\mathbf{C}_{L0}}{4} \quad (4.104)$$

The sum of the vertical tail and wing contributions gives the total

$$\mathbf{C}_{lr} = \frac{\mathbf{C}_{L0}}{4} + 2\eta_v \frac{z'_v}{b} V_v a_v \quad (4.105)$$

The yawing moment due to yaw rate is called the *yaw damping*, and also has contributions from both the vertical tail and the wing. The contribution of the vertical tail is due to the side force acting through the moment arm ℓ_v , and is analogous to that of the horizontal tail to pitch damping \mathbf{C}_{mq} . Thus, we have

$$\mathbf{C}_{nr})_V = -\frac{\ell_v}{b} \mathbf{C}_{y_r} = -2\eta_v \frac{\ell_v}{b} V_v a_v \quad (4.106)$$

The contribution of the wing to yaw damping is similar to its contribution to rolling moment, except now it is the variation of drag (rather than lift) along the span that generates the moment. Thus, if the sectional drag is also assumed to vary elliptically along the span, we find a contribution analogous to Eq. (4.104)

$$\mathbf{C}_{nr})_{\text{wing}} = -\frac{\mathbf{C}_{D0}}{4} \quad (4.107)$$

and the sum of vertical tail and wing contributions is

$$\mathbf{C}_{nr} = -\frac{\mathbf{C}_{D0}}{4} - 2\eta_v \frac{\ell_v}{b} V_v a_v \quad (4.108)$$

Derivatives with Respect to Roll Rate

The derivatives with respect to roll rate p include the side force

$$Y_p \equiv \frac{1}{m} \frac{\partial Y}{\partial p} = \frac{Q S b}{2 m u_0} \mathbf{C}_{y_p} \quad (4.109)$$

where

$$\mathbf{C}_{y_p} \equiv \frac{\partial \mathbf{C}_y}{\partial \hat{p}} \quad (4.110)$$

where $\hat{p} = pb/(2u_0)$ is the dimensionless roll rate, and the rolling moment

$$L_p \equiv \frac{1}{I_x} \frac{\partial L}{\partial p} = \frac{Q S b^2}{2 I_x u_0} \mathbf{C}_{l_p} \quad (4.111)$$

and yawing moment

$$N_p \equiv \frac{1}{I_z} \frac{\partial N}{\partial p} = \frac{Q S b^2}{2 I_z u_0} \mathbf{C}_{n_p} \quad (4.112)$$

The derivative of side force with respect to (dimensionless) roll rate \hat{p} arises from the linear distribution of perturbation angle of attack along the span of the vertical tail

$$\Delta\alpha = \frac{pz'}{u_0} = \frac{z'}{b}\hat{p} \quad (4.113)$$

where, in this equation, z' is measured from the vehicle c.g. along the *negative* z -axis. The side force is then given by

$$\Delta Y = -\eta_v Q \int_0^{b_v} c_v \left(\frac{\partial c_\ell}{\partial \alpha} \right)_v \Delta\alpha dz' = -2\eta_v Q \left(\frac{b_v}{b} \right)^2 b\hat{p} \int_0^1 \left(\frac{\partial \ell}{\partial \alpha} \right)_v \eta' d\eta' \quad (4.114)$$

If the spanwise lift curve slope distribution is approximated as elliptic,

$$\left(\frac{\partial \ell}{\partial \alpha} \right)_v = \ell_{0\alpha} \sqrt{1 - \eta'^2} \quad (4.115)$$

where

$$a_v = \frac{\partial \mathbf{C}_{L_v}}{\partial \alpha_v} = \frac{1}{S_v} \int_0^1 \ell_{0\alpha} \sqrt{1 - \eta'^2} b_v d\eta' = \frac{\pi}{4} \frac{b_v}{S_v} \ell_{0\alpha} \quad (4.116)$$

then the dimensionless side force derivative can be written

$$\mathbf{C}_{y_p} = \frac{\Delta Y}{QS\hat{p}} = -\frac{2\eta_v b}{S} \left(\frac{b_v}{b} \right)^2 \ell_{0\alpha} \int_0^1 \eta' \sqrt{1 - \eta'^2} d\eta' = -\frac{2\eta_v b}{3S} \left(\frac{b_v}{b} \right)^2 \ell_{0\alpha} \quad (4.117)$$

Equation (4.116) can then be used to express this in terms of the vertical tail lift-curve slope a_v as

$$\mathbf{C}_{y_p} = -\frac{8}{3\pi} \eta_v \left(\frac{b_v S_v}{bS} \right) a_v \quad (4.118)$$

In practice, this derivative usually is neglected, but it will be used in the estimation of the yawing moment due to roll rate later in this section.

The derivative of rolling moment with respect to (dimensionless) roll rate \mathbf{C}_{l_p} is called *roll damping*, and is due almost entirely to the wing. The roll rate imposes a linear variation in angle of attack across the wing span given, approximately, by

$$\Delta\alpha = \frac{py}{u_0} = \frac{2y}{b}\hat{p} \quad (4.119)$$

This spanwise distribution in angle of attack produces a spanwise distribution of sectional lift coefficient equal to

$$\Delta c_\ell = a_w \frac{2y}{b} \hat{p} \quad (4.120)$$

which produces a rolling moment equal to

$$\Delta L = -2Q \int_0^{b/2} c \Delta c_\ell y dy = -\frac{Qb^2 a_w}{2} \hat{p} \int_0^1 c\eta^2 d\eta \quad (4.121)$$

or

$$\mathbf{C}_{l_p} = \frac{\Delta L}{QSb\hat{p}} = -\frac{b}{2S} a_w \int_0^1 c\eta^2 d\eta \quad (4.122)$$

For an *untapered* wing,

$$\int_0^1 c\eta^2 d\eta = \frac{S}{3b} \quad (4.123)$$

so

$$\mathbf{C}_{lp} = -\frac{a_w}{6} \quad (4.124)$$

Note that, for a tapered wing, the roll damping will be somewhat less. In particular, for the elliptical spanwise loading

$$c \frac{\partial \mathbf{c}_\ell}{\partial \alpha} = \ell_{0\alpha} \sqrt{1 - \left(\frac{2y}{b}\right)^2} = \frac{4S}{\pi b} a_w \sqrt{1 - \left(\frac{2y}{b}\right)^2} \quad (4.125)$$

it can be shown⁶ that

$$\mathbf{C}_{lp} = -\frac{a_w}{8} \quad (4.126)$$

Also, for angles of attack *past the stall*, the sign of the lift curve slope is negative, and the roll damping derivative becomes positive. Thus, any tendency for the vehicle to roll will be augmented, leading to autorotation, or spinning.

The yawing moment induced by roll rate has contributions from both the vertical tail and the wing. The vertical tail contribution comes from the side force induced by roll rate acting through the moment arm ℓ_v , the distance the vertical tail aerodynamic center is aft of the vehicle center of mass. Thus,

$$\mathbf{C}_{np})_V = -\frac{\ell_v}{b} \mathbf{C}_{yp} \quad (4.127)$$

or, using Eq. (4.118), we have

$$\mathbf{C}_{np})_V = \frac{8}{3\pi} \frac{b_v}{b} V_v a_v \quad (4.128)$$

Note that although the derivative \mathbf{C}_{yp} itself often is neglected, its contribution to \mathbf{C}_{np} can be significant.

The contribution of the wing to \mathbf{C}_{np} has two components: one due to the difference in profile drag on the left and right wing panels and one due to the yawing moment caused by the effective rotation of the lift vector on either wing panel in opposite directions – i.e., to changes in induced drag. The first component depends on the details of the wing sections and the equilibrium angle of attack. Due to the roll rate, the angle attack of the right wing is increased linearly along the span, and that of the left wing is decreased linearly along the span, as shown in Eq. (4.119). Associated with these changes in lift is an increase in profile drag on the right wing and a corresponding decrease in drag on the left wing, yielding a positive yawing moment.

The induced drag effect is associated with the rotation of the lift vector at each span station through the perturbation angle of attack induced by the roll rate, as illustrated for a typical section of the right wing in Fig. 4.9. As seen in the figure, there is a change in the sectional contribution to the induced drag given by

$$\Delta \mathbf{c}_d = -\mathbf{c}_\ell \Delta \alpha = -\mathbf{c}_\ell \frac{py}{u_0} = -\mathbf{c}_\ell \left(\frac{2y}{b}\right) \hat{p} \quad (4.129)$$

It can be shown that, for an elliptical span loading, simple strip theory integration of this effect across the span gives⁷

$$(\mathbf{C}_{np})_{\text{induced}} = -\frac{\mathbf{C}_L}{8} \quad (4.130)$$

⁶See Exercise 3.

⁷See Exercise 4.

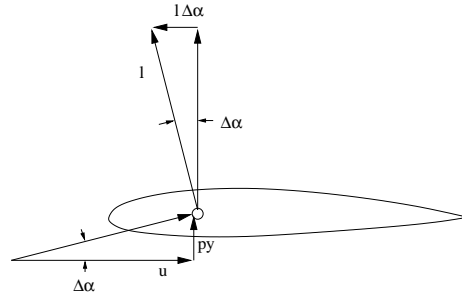


Figure 4.9: Induced drag contribution to yaw due to roll rate; the effect is illustrated for a typical section the right wing.

4.4 Control Derivatives

The control derivatives consist of the pitching moment due to elevator deflection

$$M_{\delta_e} \equiv \frac{1}{I_y} \frac{\partial M}{\partial \delta_e} = \frac{QS\bar{c}}{I_y} C_{m\delta_e} \quad (4.131)$$

the rolling moment due to aileron deflection

$$L_{\delta_a} \equiv \frac{1}{I_x} \frac{\partial L}{\partial \delta_a} = \frac{QSb}{I_x} C_{l\delta_a} \quad (4.132)$$

and the yawing moment due to rudder deflection

$$N_{\delta_r} \equiv \frac{1}{I_z} \frac{\partial N}{\partial \delta_r} = \frac{QSb}{I_z} C_{n\delta_r} \quad (4.133)$$

There also can be significant cross-coupling of the rudder and aileron control moments. The yawing moment due to aileron deflection

$$N_{\delta_a} \equiv \frac{1}{I_z} \frac{\partial N}{\partial \delta_a} = \frac{QSb}{I_z} C_{n\delta_a} \quad (4.134)$$

is called *adverse yaw*, since this derivative usually is negative, leading to a tendency to rotate the nose to the left when the vehicle rolls to the right. The rolling moment due to rudder deflection

$$L_{\delta_r} \equiv \frac{1}{I_x} \frac{\partial L}{\partial \delta_r} = \frac{QSb}{I_x} C_{l\delta_r} \quad (4.135)$$

also tends to be unfavorable, as it tends to roll the vehicle to the left when trying to turn to the right.

These control derivatives are difficult to predict accurately using simple analyses, and wind-tunnel testing or CFD analyses usually are required.

4.5 Properties of Elliptical Span Loadings

It is often useful to estimate lateral/directional stability derivatives and stability coefficients based on an elliptical spanwise load distribution. Since we usually write

$$\mathbf{C}_L = \frac{2}{S} \int_0^{b/2} \mathbf{c}c_\ell dy \quad (4.136)$$

it is clear that it is the spanwise distribution of the local chord times the section lift coefficient that is most important. Thus, we introduce

$$\ell \equiv \mathbf{c}c_\ell \quad (4.137)$$

and for an elliptical span loading we have

$$\ell = \ell_0 \sqrt{1 - \left(\frac{2y}{b}\right)^2} \quad (4.138)$$

The constant ℓ_0 is related to the wing lift coefficient by

$$\mathbf{C}_L = \frac{2}{S} \int_0^{b/2} \ell_0 \sqrt{1 - \left(\frac{2y}{b}\right)^2} dy = \frac{b\ell_0}{S} \int_0^1 \sqrt{1 - \eta^2} d\eta = \frac{\pi b\ell_0}{4S} \quad (4.139)$$

or

$$\ell_0 = \frac{4S}{\pi b} \mathbf{C}_L \quad (4.140)$$

The center of lift for a single wing panel having an elliptical span loading is then seen to be

$$\bar{y} = \frac{2}{S\mathbf{C}_L} \int_0^{b/2} y \mathbf{c}c_\ell dy = \frac{b^2}{2S\mathbf{C}_L} \int_0^1 \eta \ell_0 \sqrt{1 - \eta^2} d\eta = \frac{2b}{\pi} \int_0^1 \eta \sqrt{1 - \eta^2} d\eta = \frac{2b}{3\pi} \quad (4.141)$$

or

$$\frac{2\bar{y}}{b} = \frac{4}{3\pi} \quad (4.142)$$

That is, the center of lift of the wing panel is at approximately the 42 per cent semi-span station.

4.5.1 Useful Integrals

When estimating contributions of lifting surfaces having elliptic span loadings to various stability derivatives, integrals of the form

$$\int_0^1 \eta^n \sqrt{1 - \eta^2} d\eta \quad (4.143)$$

often need to be evaluated for various values of non-negative integer n . These integrals can be evaluated in closed form using trigonometric substitution. Thus, we have the following useful results:

$$\begin{aligned} \int_0^1 \sqrt{1 - \eta^2} d\eta &= \int_0^{\pi/2} \sqrt{1 - \sin^2 \xi} \cos \xi d\xi \\ &= \int_0^{\pi/2} \cos^2 \xi d\xi = \int_0^{\pi/2} \frac{\cos 2\xi + 1}{2} d\xi = \frac{\pi}{4} \end{aligned} \quad (4.144)$$

$$\begin{aligned} \int_0^1 \eta \sqrt{1-\eta^2} d\eta &= \int_0^{\pi/2} \sin \xi \sqrt{1-\sin^2 \xi} \cos \xi d\xi \\ &= \int_0^{\pi/2} \sin \xi \cos^2 \xi d\xi = \frac{1}{3} \end{aligned} \quad (4.145)$$

$$\begin{aligned} \int_0^1 \eta^2 \sqrt{1-\eta^2} d\eta &= \int_0^{\pi/2} \sin^2 \xi \sqrt{1-\sin^2 \xi} \cos \xi d\xi \\ &= \int_0^{\pi/2} \sin^2 \xi \cos^2 \xi d\xi = \int_0^{\pi/2} \left(\frac{\sin 2\xi}{2}\right)^2 d\xi = \int_0^{\pi/2} \frac{1-\cos 4\xi}{8} d\xi = \frac{\pi}{16} \end{aligned} \quad (4.146)$$

4.6 Exercises

1. Show that for a straight, untapered wing (i.e., one having a rectangular planform) having a constant spanwise load distribution (i.e., constant section lift coefficient), simple strip theory gives the wing contribution to the rolling moment due to yaw rate as

$$(\mathbf{C}_{l_r})_{\text{wing}} = \frac{\mathbf{C}_L}{3}$$

2. Show that for a wing having an elliptical spanwise load distribution, simple strip theory gives the wing contribution to the rolling moment due to yaw rate as

$$(\mathbf{C}_{l_r})_{\text{wing}} = \frac{\mathbf{C}_L}{4}$$

Explain, in simple terms, why this value is smaller than that computed in Exercise 1.

3. Show that the contribution to roll damping of a wing having an elliptical span loading is

$$\mathbf{C}_{l_p} = -\frac{a_w}{8}$$

4. Show that for a wing having an elliptical spanwise load distribution, simple strip theory gives the induced drag contribution of the wing to the yawing moment due to roll rate as

$$(\mathbf{C}_{n_p})_{\text{wing}} = -\frac{\mathbf{C}_L}{8}$$

Bibliography

- [1] Bernard Etkin & Lloyd Duff Reid, **Dynamics of Flight, Stability and Control**, McGraw-Hill, Third Edition, 1996.
- [2] Robert C. Nelson, **Aircraft Stability and Automatic Control**, McGraw-Hill, Second edition, 1998.
- [3] Louis V. Schmidt, **Introduction to Aircraft Flight Dynamics**, AIAA Education Series, 1998.